ISSN: 2456-9348
Vol (01) _Issue (12) Impact Factor: 4.520

iJETRM
International Journal of Engineering Technology Research & Management

EVALUATION OF THERMAL DIFFUSIVITY IN CERAMIC BLOCKS USING INFRARED THERMOGRAPHY

Researcher: Paula Glória Barbosa
Department of Science and Technology
Instituto Federal de Educação Ciência e Tecnologia de Minas Gerais, Brasil

Researcher: Caroline Rodrigues
Department of Materials Engineering
Universidade Federal de Minas Gerais, Brasil

Researcher: Cristiane do Bom Conselho Sales Alvarenga
Department of Materials Engineering
Universidade Federal de Minas Gerais, Brasil

Prof. Dr. Roberto Márcio de Andrade
Department of Mechanical Engineering
Universidade Federal de Minas Gerais, Brasil

Prof. Dr[a]: Maria Teresa Paulino Aguilar
Department of Materials Engineering
Universidade Federal de Minas Gerais, Brasil

Prof. Dr[a]: Rosemary do Bom Conselho Sales
Department of Planning and Configuration, School of Design
Universidade do Estado de Minas Gerais
rosemary.sales@uemg.br

ABSTRACT
The inadequacy of materials and architectural elements to adapt to local climatic aspects requires the use of air conditioning systems to meet human comfort and energy efficiency needs in buildings. Knowledge of the thermal properties of materials is directly related to the planning of thermal comfort and energy efficiency. In analyses of problems involving nonstationary regimes, such as in heat exchange processes that occur in the building envelope, thermal diffusivity is an important property to be considered. This study evaluated the thermal diffusivity of flat components commonly used for masonry forming, solid red clay blocks and hollow blocks made of red clay and concrete, using infrared thermography. The calculations were based on a unidimensional heat transfer model in a system subjected to a transient regime. The data were computed by the semi-infinite solid model and were validated by comparison with values from published works. The results indicated that infrared thermography is a suitable technique to characterize the thermal diffusivity of building materials.

Keywords: Infrared Thermography, Thermal Diffusivity, Energy Efficiency, Ceramic Blocks.

INTRODUCTION

The comfort of the built environment is an important parameter in planning constructions that are appropriate from the thermal point of view. This factor defines the mental state that expresses people's satisfaction with the environments they inhabit [1], [2],[3],[4]. The thermal performance of buildings, on the other hand, is directly related to the properties of materials.

Thermal diffusivity is an important property for evaluating the performance of systems that undergo heating and/or cooling processes. This property expresses how quickly a body completely adjusts to the temperature of

the surrounding area and how much it depends on the speed of energy propagation inside the material (thermal conductivity) and its volumetric specific heat. Thus, both diffusivity and conductivity are important variables for the thermal control of buildings [5].

The materials used for masonry forming have a sealing function. Accordingly, they greatly contribute to the comfort inside buildings. A study of diffusivity associated with the characterization of building materials would allow better assessment of their heat-conduction capabilities in relation to their thermal energy storage capacity. For high thermal diffusivity values, the material quickly responds to changes in the outside temperature, which in the case of a building, causes rapid changes in internal temperature, and may be uncomfortable under certain climatic conditions. On the other hand, low-diffusivity materials retard the transfer of external temperature variations into the interior of buildings, thus contributing to the thermal comfort.

A non-destructive testing technique called thermography allows for measuring surface temperatures without direct contact with them. This technique has been being used in investigations involving the heat transfer phenomena, using devices that convert thermal energy into electrical pulses that, after processing, appear as digital images to represent the temperature profile of any surface [6],[7]. Currently, studies and practical applications of thermography are being directed toward civil engineering needs, with a view to identifying heat losses in building envelopes and the visualization of inhomogeneities and defects close to the surface of concrete and in historical masonry structures [8], [9], [10], [11]. Several studies address the use of thermography for the thermal characterization of materials and the determination of thermal diffusivity [12], [13], [14], [15], [16], [6], [17], [18], [19]. However, no papers were given addressing the use of thermography to analyze the thermal properties of hollow blocks, generally used for masonry, or even solid blocks. In order to contribute to the knowledge, it is proposed a new experimental technique for measuring the thermal diffusivity of solid and hollow blocks of ceramic material (red clay and concrete) using infrared thermography and the mixture rule. The method considers unidimensional heat transfer in a system subjected to a transient regime. The data were stored and analyzed using the semi-infinite solid model and were compared to the theoretical values relative to the material's thermal diffusivity.

THEORETICAL FOUNDATIONS

Thermal diffusivity is defined by the ability of a material to conduct thermal energy in comparison to its ability to store it. In other words, it concerns the speed at which the body completely adapts to the temperature of its surroundings [20]. It is determined by the ratio of thermal conductivity and volumetric heat capacity:

$$\alpha = \frac{k}{\rho . c_p} \tag{1}$$

where,
α = denotes thermal diffusivity (m^2/s)
k = stands for thermal conductivity (W/mK)
ρ = represents density (kg/m^3)
c_p = is the specific heat at the material's constant pressure (J/kg.K)

The heat-diffusion equation for a transient unidirectional conduction considering the thermal conductivity as constant is given by:

$$\frac{\partial^2 T}{\partial x^2} = \frac{1}{\alpha}\frac{\partial T}{\partial t} \tag{2}$$

Where,
T is the solid temperature (°C)
x = is the direction in which heat transfer occurs
t = stands for time (seconds)

iJETRM
International Journal of Engineering Technology Research & Management

The analytical solution for Eq. 2 depends upon the solid geometry through which the heat flux takes place. The geometry of a semi-infinite solid is simple. According to the literature, it can be used in idealizations that analyze the finite-dimensional solid provided that the perturbation of temperature in one face does not reach the opposite face in the considered time interval. For this model to be fitted to the studied situation, the minimum temperature variation on the opposite side was considered when the value exceeded the measurement uncertainty [20]. When considering a semi-infinite solid subjected to a constant flow of thermal energy applied in a recognizable surface (boundary condition of the second kind), the solution of equation 2 is given by [20]:

$$T(x,t) - Ti = \frac{2.q_O''\sqrt{(\alpha t/\pi)}}{k}\exp\left(\frac{-x^2}{4\alpha t}\right) - \frac{q_O'' x}{k} erfc\left(\frac{x}{2\sqrt{\alpha t}}\right) \quad (3)$$

Where,
$T(x,t)$ = represents the surface temperature that varies with time (°C)
Ti = is the surface temperature at the initial time (°C)
q_o'' is the surface heat flux (W/m²)
α = stands for thermal diffusivity (m²/s)
t = symbolizes time in seconds
k = means thermal conductivity (W/mK)
x = is the distance from the material's surface (m)

The complementary error function *(erfc),* in turn, is calculated from $erfc(w) = 1 - erf(w)$, where *erf (w)* is the Gauss error function. Thus, knowing the geometry and temperature variation of the solid surface with time allows for evaluating the thermal diffusivity using the above equations, whose resolution requires interpolation and interaction.

MATERIALS & METHODS

3.1. Material

The analyzed materials were solid blocks of red clay and hollow blocks of red clay and concrete, whose characteristics are shown in Table 1.

Table 1 - Characteristics of the used materials.

Block Description	Macrostructure	Dimensions (m^3)	Compression strength (MPa)	Density kg/m^3
Solid red clay		0.22 × 0.011 × 0.55	1.5	1400
Hollow red clay		0.39 × 0.19 × 0.09	4.5	1300
		0.39 × 0.19 × 0.14	4.5	1320
		0.39 × 0.19 × 0.19	4.5	1350
Hollow concrete		0.39 × 0.19 × 0.09	3	2280
		0.39 × 0.19 × 0.14	4	2285
		0.39 × 0.19 × 0.19	3	2310

iJETRM
International Journal of Engineering Technology Research & Management

For the evaluation of the blocks' thermal diffusivity, was have used infrared thermography and mathematical modeling. This method was originally validated using solid red clay blocks, since there are published works with experimental results relative to these materials. At the second stage, the measurement uncertainties were evaluated. At the third stage, the theoretical–experimental method validated for solid red clay blocks was used to estimate the thermal diffusivity of red clay and concrete hollow blocks.

3.2 Method

3.2.1 Evaluation of the thermal diffusivity of solid red clay blocks.

The solid red clay blocks' diffusivity was evaluated based on the one-dimensional mathematical model of heat transfer in a transient regime to a semi-infinite solid. In this regard, it was necessary to experimentally determine the blocks' surface temperature variation under the experimental conditions relevant to the theoretical model, where: the analysis position x corresponds to the block's thickness, the constant heat flow is generated by a halogen lamp (127 V) of 1,000 W output power, which can be quantified owing to a sealing condition that prevents thermal energy loss to the environment, and the reading of the block's surface temperature is conducted by a thermocamera.

The experiment consisted of subjecting the solid red clay block to the heat generated by the lamp and monitoring the temperature of its outer surface for 1 h. The warming occurred within an insulated box of dimensions 0.47 × 0.70 × 0.27 m3 (Figure 1). The sample was positioned in front of the box and was sealed at the top, with one of the surfaces in contact with the heat flow while another surface was exposed for temperature reading.

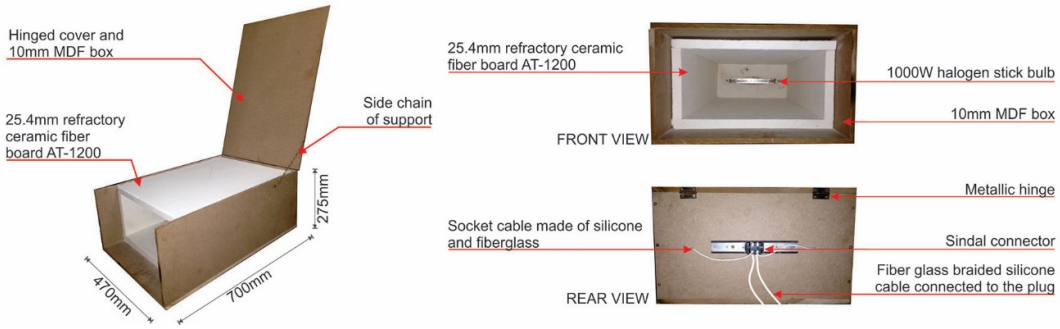

Figure 1: Thermal box for heating blocks

The box was composed of medium density fiberboard (MDF) of thickness 10 mm. Fixing screws, metal hinges, and compression lever latches to articulate/seal the lid were used in the assembly. In order to avoid heat losses by propagation, the inside of the box was coated with insulating plates of Texfiber AT-1200 (25.4 mm thickness). A preliminary analysis of thermograms of the block revealed that the box's sealing system was effective, significant impeding the leakage of thermal energy from inside.

It was necessary to set up the thermocamera for monitoring the temperature in such a way as to adjust the focus, set the temperature scale, and edit the inputs (emissivity, object distance, reflected temperature, atmospheric temperature, and relative humidity).

The emissivity of the red clay block was estimated by the known temperature technique: the procedure is carried out based on the temperature of the material via thermocouple, and the variation of the emissivity value, as determined by the camera's thermal imager, until it reaches a value corresponding to the temperature read by the thermocouple. Five points were analyzed and the mean emissivity and the standard deviation were calculated.

The thermography equipment was positioned 0.9 m away from the block's outer surface and was programmed to record images at intervals of 1 min. The atmospheric temperature and relative humidity were measured by a thermohygrometer NTC -10 (Testo 622) at 60 °C with humidity 0 at 100% rF and pressure of 300–1200 hPa.

It is noteworthy that the heat flow qo" propagated into the internal surface of the block is the total amount of heat emitted by the lamp. Regarded as a diffuse surface, the lamp emits heat in the form of radiation in all

directions. The total rate at which radiation leaves the lamp and is intercepted by the block surface is influenced by the geometric characteristics of the surfaces. This influence is quantified by the form factor Fij. The amount of heat absorbed by the block surface can then be calculated by the expression:

$$q_o" = F_{ij} \frac{Pot}{A} \quad (4)$$

where,
$q_o"$ = is the heat rate intercepted by the block surface (W/m$^{2)}$
Pot = is the heat rate emitted by the lamp (W),
A = is the block's surface area (m^2)
F_{ij} = is the form factor between the surfaces of the lamp and the block

To determine the shape factor between the lamp and the block, we have adopted a relationship where settings - parallel cylinder and rectangle - are considered infinitely long and therefore two-dimensional [20], and the computer program *Engineering Equation Solver (EES)* has been used to solve the mathematical model.
The thermocouple rods were coupled in the inner and outer faces of the red clay block using an adhesive tape (Figure 2). The readings were carried out using two terminals of the thermocouples connected to the data acquisition system at the inner and outer surfaces.

Figure 2: Fixation of the thermocouple rods in the inner and outer faces of the red clay block using an adhesive tape.

The data collection consisted of monitoring the temperature of the block's outer surface, while its inner surface was subjected to the constant heat flow emitted by the lamp. Aiming to assess a region free from thermal interferences, the temperature of a central area of the block was analyzed. Values from the surface temperature obtained by thermography were treated as input values for Equation 3, as well as the time, in seconds, while the diffusivity α was an output variable. The computer program solved the mathematical model. The block's thermal conductivity, which is necessary for the solution of the equation, was determined by the energy compensation method in a preliminary work.

The temperatures recorded by the thermocamera were considered. By means of thermograms, one can calculate the average surface temperature in a given block area for each point in time.

3.3. Uncertainty analysis

The uncertainty analysis considered interferences generated in the indirect measurement of temperature by thermal imaging and the mathematical modeling for semi-infinite solids. Regarding the indirect temperature measurement process by thermography, the magnitudes associated with measurement uncertainty are the emissivity at room temperature, reflected temperature, distance between the tested object and the equipment, and signal from the thermocamera [17].

The uncertainty in emissivity is assumed to be the standard deviation of emissivity values measured at five different points across the sample. With respect to the ambient temperature and the reflected temperature, we have used the uncertainty value reported by the thermo hygro-clock's manufacturer. The uncertainty assigned to the distance between the thermocamera and the block's outer surface is also related to the measuring instrument, which was, in this case, a metric tape graduated in millimeters. According to the specific literature, the uncertainty of a graduated instrument is the half of its resolution [21]. Nonetheless, for this experiment, we

iJETRM
International Journal of Engineering Technology Research & Management

adopted a conservative approach owing to the difficulty of obtaining the exact point of the thermocamera's lens, assuming a value greater than 0.5 mm. The uncertainty value from the thermocamera's signal was based on the work conducted by [23], which assesses the uncertainty of a point considered relevant from each of the thermograms. The uncertainty range generated in the test with the solid red clay blocks was considered in the other experiments, since the uncertainty ranges of the input parameters match the temperature variation, which is relatively low in order that their values vary.

In the mathematical model used, the quantities associated to the uncertainty of the thermal diffusivity were heat flow, thermal conductivity, thickness of the block, temperature, and time. The temperature uncertainty value was obtained from the above procedure. Nevertheless, the heat flow generated by the lamp has no known uncertainty and the literature does not provide a method for determining it. The conductivity value was considered constant for each block. These parameters were estimated with 10% uncertainty. The value of block thickness was assumed to be an uncertainty equal to half the resolution of the graduated scale, whereas time was associated with temperature, since its determining criterion was the temperature variation captured by the thermocamera. From these data, the uncertainty range of thermal diffusivity values were calculated using the EES software.

3.4. Evaluation of the thermal diffusivity of ceramic hollow blocks

The data were collected and treated similarly those of the solid red clay block. The tests were conducted to make measurements until the time a variation of 2 °C was reached between the opposing faces of the blocks. Thus, the heating times of the samples ranged from 1350 to 2020 s. The thermal conductivity of the hollow blocks was determined using the conductivity value of the material, the rule of mixtures, and considering that the blocks were composed of air and solid material (red clay or concrete). Determination of the equivalent thermal conductivity began with the dimensional analysis of blocks (Figures 3 and 4). The thicknesses of air layers in the concrete blocks of 90, 140 and 190 mm are, respectively, 50, 100, and 150 mm. The red clay plates, on the other hand, have a varying internal geometry.

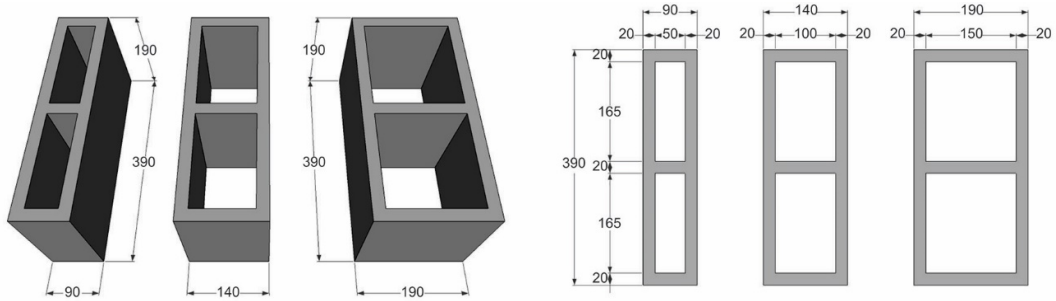

Figure 3: Considered dimensions of the concrete blocks.

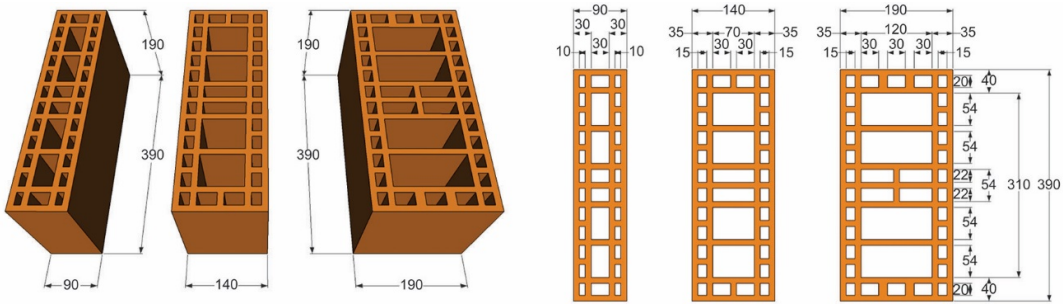

Figure 4: Considered dimensions of the red clay blocks.

iJETRM
International Journal of Engineering Technology Research & Management

After a dimensional analysis of the blocks, the equivalent thermal conductivity of each sample has been determined, as shown in Equation 4 by the calculation of the equivalent thermal conductivity of the 90-mm-thick concrete block (Figure 5).

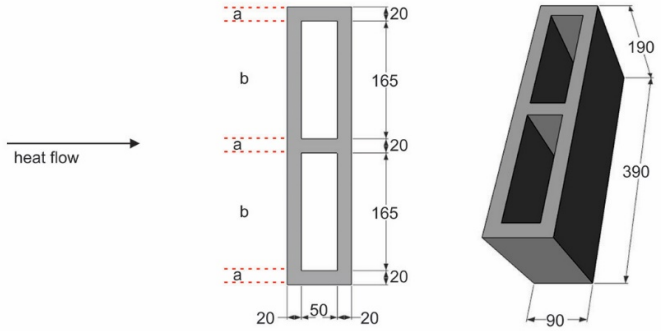

Figure 5: Calculation of equivalent thermal conductivity of the concrete block.

Section a: homogeneous concrete layer
Section b: inhomogeneous layer made of concrete + air + concrete
Aa = 0.02m x 0.19m = 0,0038m2
Ab = 0.165m x 0.19m = 0,3135m2

$$R_t = \frac{0{,}09\ m}{1{,}75\ W/mk} = 1{,}076\ m^2.k/W$$

$$R_t = \frac{3Aa + 2Ab}{3Aa + 2Ab} = 1{,}076\ m^2.k/W$$

$$Ra \rightarrow Rb \qquad (5)$$

$$R_b = \frac{0{,}02}{1{,}75} = \frac{0{,}05}{0{,}03} + 1{,}698\ m^2.k/W$$

$$R = \frac{e}{k} k_t = \frac{e}{r_1} = \frac{0{,}09}{1{,}076}$$

$$k_t = 0{,}084\ W/m.k$$

DATA ANALYSIS AND FINDINGS.

4.1. Evaluation of the thermal diffusivity of solid red clay blocks.

Figure 6 shows the temperature variation recorded by the thermocouple of the inner and outer faces of the massive red clay block over the first 1100 s of heating. The temperature of the block's inner face increases monotonically in the ranges of 0–410 and 500–1100 seconds. The observed inflection of around 410 s could be related to the partial detachment of the thermocouple's rod in the block's inner surface, owing to the high temperature. The temperature variation on the outer surface is not discernible in the scale represented in the chart.

iJETRM
International Journal of Engineering Technology Research & Management

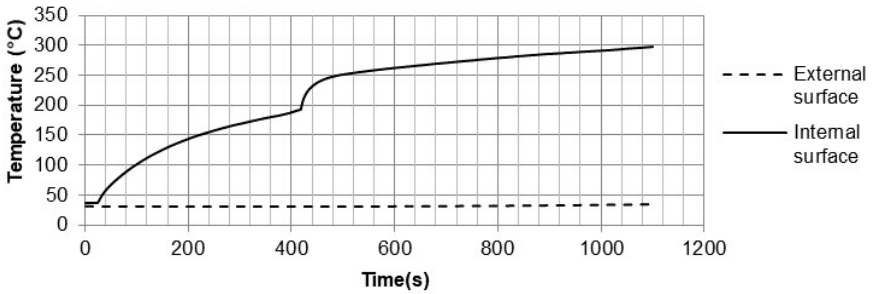

Figure 6: Internal and external temperature of the solid red clay block.

Figure 7 shows the thermal behavior of the solid block's outer surface with an extended scale. In the time interval between 0 and 1030 s, the temperature ranged from 31.5 to 33.5 °C, a visible increase of 2 °C. As a semi-infinite solid has a geometry in which the changes imposed to its identifiable surface are not observed on the opposite surface [20], the variation observed in the present study corroborates the hypothesis that the studied block has such geometry.

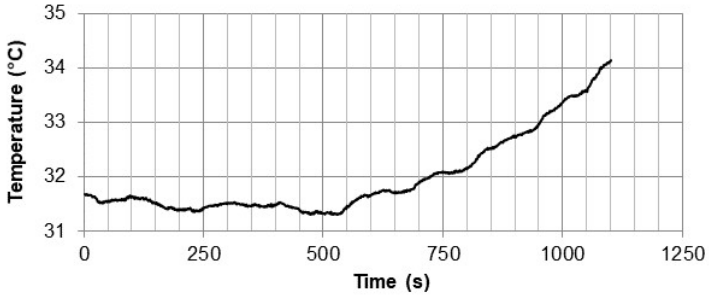

Figure 7: External temperature of the solid red clay block.

The emissivity of the solid red clay block obtained using the method of known temperature, as well as the input data for thermographic analyses are presented in Table 2.

Table 2 – Input parameters of the thermocamera.

Parameters	Emissivity	Distance of object (m)	Atmospheric temperature (°C)	Relative unit (%)
Values	0.95	0.9 m	23.3	73%

Figure 8 shows the average temperature values recorded over time and obtained by thermogram analysis of the block's outer face. We observed that the temperature remained constant until nearly 380 s, when a visible temperature increase began, having reached about 27.1 ºC at 660 s. We observed an inconsistency in the reading of temperature during the 380 s, including a decrease in values. This occurred due to a physical phenomenon where the temperature should be stable or tend to increase. Such a disruption may have been due to the reading instability of the thermocamera with the tool "area", once this feature calculates the average temperature of each thermogram pixel.

iJETRM
International Journal of Engineering Technology Research & Management

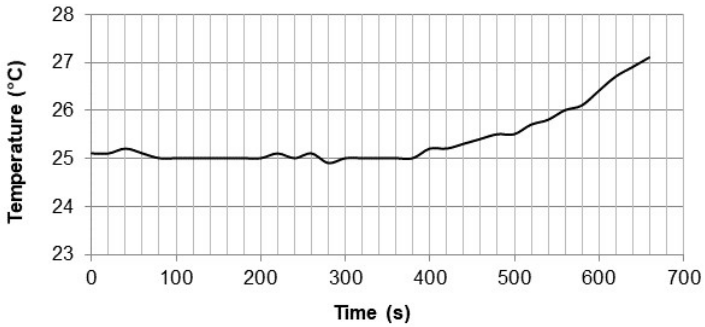

Figure 8: Temperature variation of the solid red clay block as verified by thermography.

Values of the same order were recorded by the thermocouple. Thus, the initial temperature was considered to be 25 °C, given by the average temperature measured by thermography during the first 380 s of the test. To calculate the diffusivity of the semi-infinite solid, according to the Equation 2, the following parameters have also been used: block thickness of 0.055 m and thermal conductivity of 0.7 W/mK. The conductivity value obtained by the energy compensation method is similar to that reported in the literature by Ashby, 2011 (22). The heat flow was calculated by Equation 4, considering the value of 0.02475 m² for the surface of contact with the heat flow, and the power of 1000 W for the lamp supplied by the manufacturer, a form factor of 0.601 (with input parameters of 0.01: distance between the center of the lamp and the block's inner face, and 0.055 m: half the height of the block). The calculated value was then 6468.69 W/m².

From these data, we evaluated the behavior of thermal diffusivity throughout the block-heating process (Figure 9). The thermal diffusivity values were observed to decrease markedly during the first 100 s period, after which there was a tendency for the diffusivity values to level out, which remained almost constant from 400 s onwards. By analyzing Equation 3, which describes the temperature profile of the behavior in a semi-infinite solid in terms of time and position, it is clear that in the first member there is a subtraction between the temperature value at position (x) and at time (t), and the value of the initial temperature (Ti). Once the sample's outer face temperature - where (x) is the thickness of the block - remained constant during the first 600 s and equal to (Ti), the subtraction result is zero and, as the other variables remained constant, except for the time, a decrease in the diffusivity values was expected.

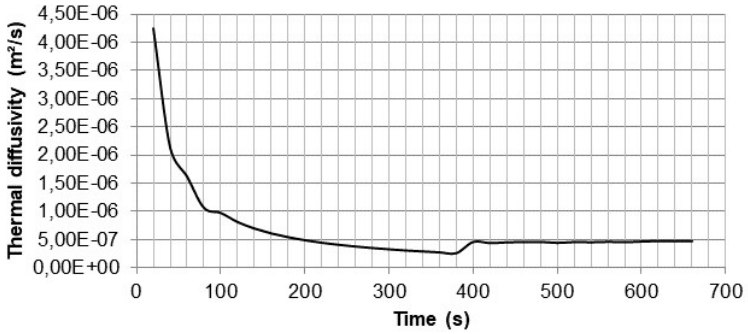

Figure 9: Thermal diffusivity behavior of the solid red clay block over time.

4.2. Uncertainty analysis

The uncertainty relative to the mediated emissivity was 0.05. In relation to the ambient temperature and the reflected temperature, the uncertainty was 1°C. An uncertainty of 0.01 m was assumed for the measurement of the distance between the thermocamera and the block's outer surface. The thermal imager signal had uncertainty of 0.7 V. From these data, we determined the uncertainty in temperature measurements for each point chosen at each of the 34 thermograms from the solid red clay blocks. We opted for the expanded uncertainty from the GUM method [23], corresponding in this case to 3.9%. Given the proximity of the uncertainty values obtained at each of the points of the analyzed thermograms, it was decided that the temperature measurement uncertainty

would be 4% - the highest of the values found - and this value was also considered for the other trials. The graph in Figure 10 shows the temperature values recorded by thermography with its respective uncertainty bands.

In calculating the uncertainty of the thermal diffusivity, 1 °C was defined as the temperature reading uncertainty, which corresponds to 4% of the temperature in the analyzed range. For the parameters heat flow and thermal conductivity, the uncertainty was estimated at 10%, i.e., 646.87 W/m² and 0.072 W/mK, respectively.

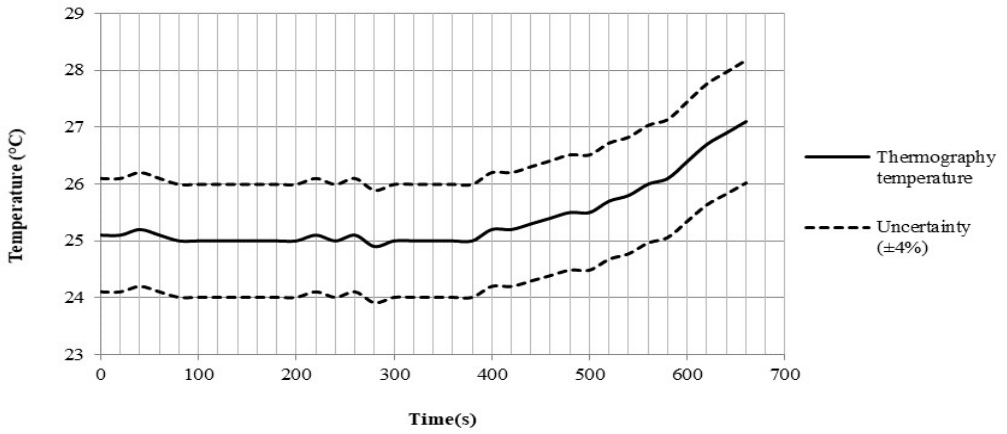

Figure 10: Temperature variation over time and corresponding uncertainty range.

The uncertainty for the thickness value was 0.0005 mm, whereas the uncertainty for the time was 1 s. Figure 11 shows the variation in thermal diffusivity in the solid block over time, as well as the range of uncertainty assigned to the measurement process. We note that the uncertainty values decrease over time, tending towards very similar values. Moreover, we have observed that in the interval between 40 and 420 s, uncertainty suggests negative values for diffusivity, which, of course, should be disregarded, since only positive values can be assigned to this property.

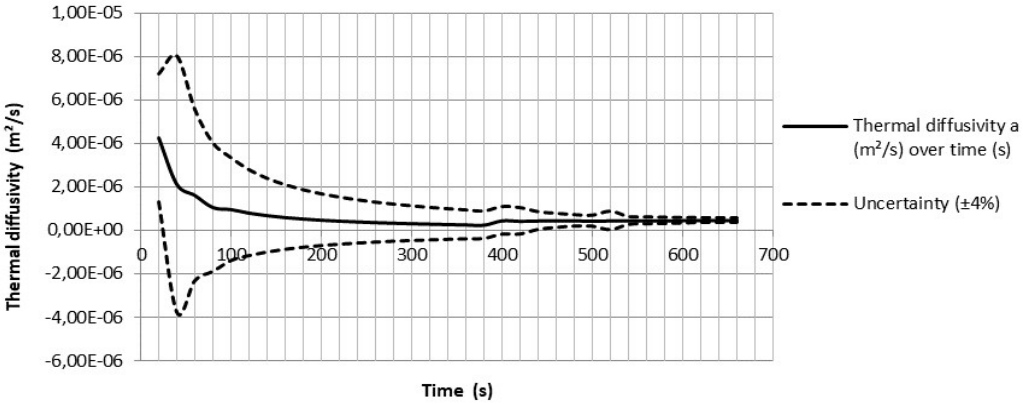

Figure 11: Diffusivity variation over time and corresponding uncertainty range.

Incropera and DeWitt [20] reported that the diffusivity of the solid red clay block is 4.49×10^{-7} m²/s, i.e., within the uncertainty range of the value obtained experimentally, which is $(4.68 \pm 0.8) \times 10^{-7}$ m²/s. These data indicate that the experimental model is suitable and applicable to the analysis of thermal diffusivity of ceramic component of flat surfaces.

4.3. Evaluation of the thermal diffusivity of red clay and concrete hollow blocks.

The emissivity of hollow blocks obtained using the method of known temperature, as well as the

iJETRM
International Journal of Engineering Technology Research & Management

input data for thermographic analyses are presented in Table 3.

Table 3 – Input parameters of the thermocamera.

Parameters	Hollow red clay block			Hollow concrete block		
Measure of blocks (m)	0.09	0.14	0.19	0.09	0.14	0.19
Emissivity	0.95	0.95	0.95	0.9	0.9	0.9
Distance of object (m)	0.9	0.9	0.9	0.9	0.9	0.9
Atmospheric temperature (°C)	22.8	24.0	24.5	24.3	23.6	22
Relative unit (%)	72	60	52	62	57	63

The average temperature profile of the external faces of the hollow blocks obtained by thermography during the heating process is shown in Figure 12. Here, the point from which one can observe the heating face (dead time) is emphasized.

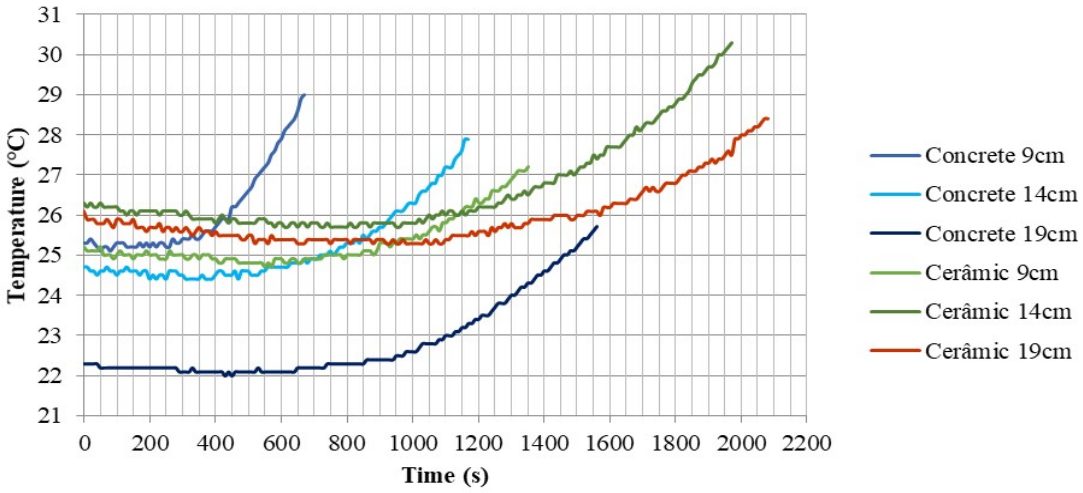

Figure 12: Temperature as a function of time for three tests with concrete/red clay hollow blocks.

By observing the curves on the graph, one can conclude that, for the hollow red clay block, the smaller the thickness of the sample, the smaller the dead time of the respective heating process, and thus more quickly the temperature changes can be perceived on the outer surface. It is clear, also, that the curves show the same tendency, only varying the speed of the heating process of each block.

As it was noted for the hollow red clay blocks, the smaller the thickness of the hollow concrete block, the smaller the dead time of the respective heating process, and thus the more quickly the temperature changes can be perceived on the outer surface. It is clear, also, that the curves have the same tendency, only varying the speed of the heating process. It should be emphasized, though, that this tendency is different from that observed for the hollow red clay blocks.

By comparing the mean external surface temperature profiles of both red clay and concrete blocks during the heating process, one might conclude that the outer surfaces of hollow concrete blocks are subjected to faster temperature variations on their inner surfaces.

To calculate the diffusivity, we have adopted the same methodology used for massive blocks, differing only in determining the conductivity. Because these were hollow blocks, we have calculated the equivalent thermal conductivity of each sample using the rule of mixtures, since the blocks consist of homogeneous layers of concrete or ceramic, and air layers (Table 4).

iJETRM
International Journal of Engineering Technology Research & Management

Table 4 – Values for total thermal resistance and equivalent thermal conductivity of the samples.

Block	Thickness (mm)	Conductivity (W/mK)
Red clay	90	0.210
	140	0.200
	190	0.197
Concrete	90	0.314
	140	0.305
	190	0.301

The results indicate that the equivalent thermal conductivity of the hollow red clay blocks is lower when compared to those obtained for the hollow concrete blocks. This result was expected, since the thermal conductivity of concrete is greater than that of ceramics [22]. These results corroborate those reported in Figures 13: If the hollow concrete blocks heat proportionally faster as compared to hollow red clay blocks, the values of their equivalent thermal conductivities should be higher.

The thermal diffusivity values of the samples during the heating process of hollow red clay blocks obtained with the EES tool are shown in Figure 13. The curves are observed to have the same behavior, tending to a constant value, as observed in the diffusivity graph as a function of the time for the test with the solid ceramic block.

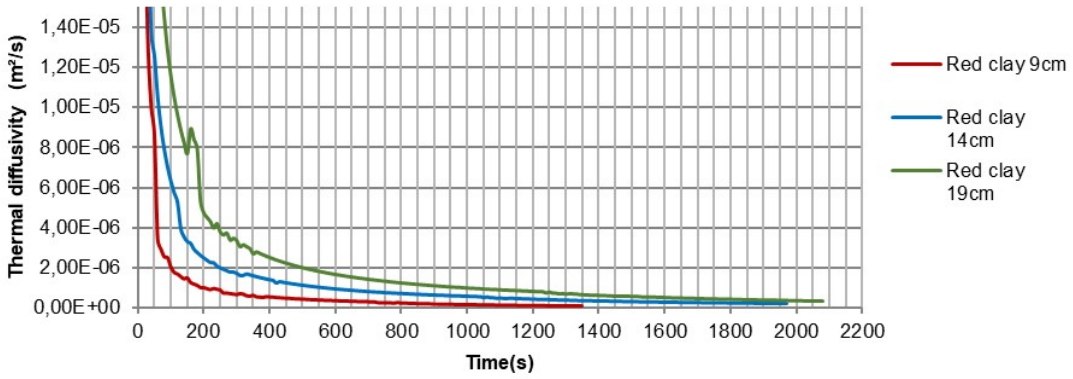

Figure 13: Thermal Diffusivity versus time of the hollow red clay blocks.

Figure 14 shows the results obtained for the hollow concrete blocks. The curves relative to both the solid red clay blocks and the hollow red clay blocks exhibit the same behavior, while the thermal diffusivity values tend to be constant over time.

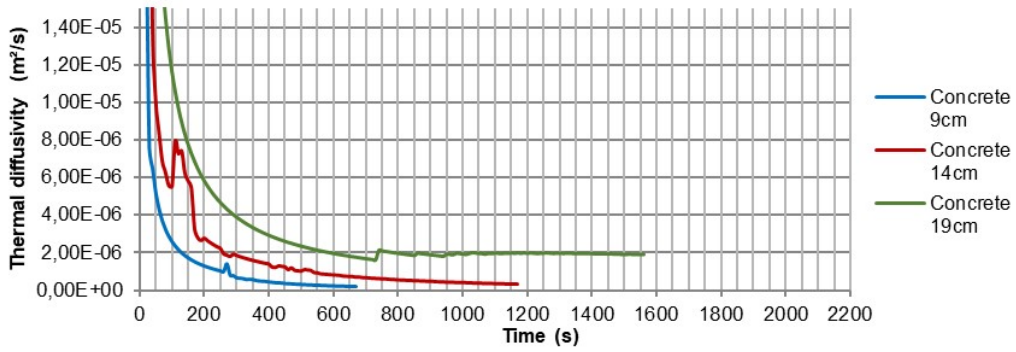

Figure 14: Thermal Diffusivity as a function of the time of hollow concrete blocks.

Table 5 shows the thermal diffusivity values of the concrete and red clay hollow blocks after the diffusivity is stabilized.

Table 5 – Last thermal diffusivity values found for each sample.

Block	Thickness (mm)	Diffusivity (m^2/s)
Solid red clay	-	$4{,}68 \times 10^{-7}$
Hollow red clay	90	$1{,}14 \times 10^{-7}$
	140	$1{,}85 \times 10^{-7}$
	190	$3{,}57 \times 10^{-7}$
Hollow concrete	90	$2{,}00 \times 10^{-7}$
	140	$3{,}03 \times 10^{-7}$
	190	$1{,}88 \times 10^{-6}$

The thermal diffusivity obtained for the solid red clay block has the largest value. The values obtained for the compounds are smaller, as a result of the air layers, since the thermal conductivity of air is approximately 27.4 times lower than that of ceramics and 66.5 times lower than that of concrete.

Altogether, the diffusivity values of the hollow red clay blocks are smaller than those obtained for their concrete counterparts. This result indicates that hollow red clay blocks have a response time to temperature changes determined by their surroundings below that of the hollow concrete blocks. The same tendency is observed for blocks of the same nature: The smaller the thickness, the lower the thermal diffusivity, due to a greater barrier to heat flow.

CONCLUSIONS

The main contribution of this study is that the thermal diffusivity of ceramic blocks, solid and hollow blocks, can be estimated by the technique of infrared thermography.

The value obtained for diffusivity of solid block was similar to that described in the literature, with the difference lying in the uncertainty range of the value obtained experimentally.

The results of this study lead to the conclusion that, with respect to contributing to a comfortable ambience inside the buildings, the solid red clay blocks are less suitable for forming the walls than the red clay and concrete hollow blocks, since their diffusivity is higher than those of the others. It is believed that the contribution of air layers of hollow blocks is crucial to the end result.

When comparing hollow blocks of same thickness, we have found that those produced with red clay and air have lower values of thermal diffusivity than hollow concrete blocks. In conclusion, it is believed that, since the response time of the hollow red clay blocks to temperature changes imposed by the surroundings are below that of the hollow concrete blocks, they are more suitable in climate conditions where reducing the daily temperature range is strategic to obtain the thermal conditions optimal for a comfortable ambience inside the built environment.

Nevertheless, we believe that the tendency presented in blocks of similar nature in regard to their thickness – the smaller the thickness, the lower the thermal diffusivity – is a matter to be addressed in future works.

ACKNOWLEDGEMENTS

This work was supported by the Coordination for the Improvement of Higher Education Personnel (CAPES); the Research Support Foundation of the State of Minas Gerais (FAPEMIG); the National Council for Scientific and Technological Development (CNPq).

iJETRM
International Journal of Engineering Technology Research & Management

REFERENCES

[1] Aghniaey, S.; Lawrence, T. M; Mohammadpour, J.; Song, W.; Watson, R.T and Boudreau, M. C. *Optimizing thermal comfort considerations with electrical demand response program implementation*. Journal of Building Services Engineering Research & Technology 39(2), 2018 pp.201-231, doi: 10.1177/0143624417752645.

[2] Ali, S. A.; Chua, S. J. L.; Lim, M. E. *The effect of physical environment comfort on employees' performance in office buildings. A case study of three public universities in Malaysia*. Structural Survey. Vol. 33 Issue: 4/5, (2015), pp.294-308, https://doi.org/10.1108/SS-02-2015-0012.

[3] Manzano-Agugliaro F, Montoya FG, Sabio-Ortega A, García-Cruz A. *Review of bioclimatic architecture strategies for achieving thermal comfort.* Renew Sustain Energy Rev 2015;49:736–55. doi: 10.1016/j. rser.2015.04.095.

[4] Nico MA, Liuzzi S, Stefanizzi P. *Evaluation of thermal comfort in university classrooms through objective approach and subjective preference analysis*. Appl Ergon 2015; 48:111-20. doi:10.1016/j.apergo.2014.11.013.

[5] Evola, G.; Marletta, L.; Sicurella, F. *Simulation of a ventilated cavity to enhance the effectiveness of PCM wallboards for summer thermal comfort in buildings*. Energy and Buildings Volume 70, February 2014, Pages 480-489. doi.org/10.1016/j.enbuild.2013.11.089.

[6] Vavilov VP, Pawar S. *A novel approach for one-sided thermal nondestructive testing of composites by using infrared thermography*. Polym Test 2015; 44:224-33. doi:10.1016/j.polymertesting.2015.04.013.

[7] Kylili A, Fokaides PA, Christou P, Kalogirou SA. *Infrared thermography (IRT) applications for building diagnostics: A review*. Appl Energy 2014; 134:531-49. doi:10.1016/j.apenergy.2014.08.005.

[8] Lucchi, E. *Applications of the infrared thermography in the energy audit of buildings: A review.* Renewable and Sustainable Energy Reviews 82 (2018) 3077–3090.

[9] Lourenço, T.; Matias, L.; Faria,P. *Anomalies detection in adhesive wall tiling systems by infrared thermography*. Construction and Building Materials 148 (2017) 419–428.

[10] Tejedor, B.; Casals, M.; Gangolells, M.; Roca, X. *Quantitative internal infrared thermography for determining in-situthermal behaviour of facades*. Energy and Buildings 151 (2017) 187–197.

[11] Meola, C. *Infrared Thermography in the Architectural Field*. Hindawi Publishing Corporation. The ScientificWorld Journal.Volume 2013, Article ID 323948. http://dx.doi.org/10.1155/2013/323948.

[12] Wakili, K. G.; Dworatzyk,C.; Sanner, M.; Sengespeick, A.; Paronen, M.; Stahl, T. *Energy efficient retrofit of a prefabricated concrete panel building (Plattenbau) in Berlin by applying an aerogel based rendering to its façades*. Energy & Buildings 165 (2018) 293–300.

[13] Khoukhi, M. *The combined effect of heat and moisture transfer dependent thermal conductivity of polystyrene insulation material: Impact on building energy performance*. Energy & Buildings 169 (2018) 228–235.

[14] Cifuentes, A.; Mendioroz, A.; Salazar, A. *Simultaneous measurements of the thermal diffusivity and conductivity of thermal insulators using lock-in infrared thermography*. International Journal of Thermal Sciences 121 (2017) pp.305 e 312.

[15] Basheer, C.M.; Krishnamurthy, C.V.; Balasubramaniam, K. *Hot-rod thermography for in-plane thermal diffusivity measurement*. Measurement 103 (2017) 235–240.

[16] Pech-May N. W, Mendioroz A, Salazar A. *Simultaneous measurement of the in-plane and in-depth thermal diffusivity of solids using pulsed infrared thermography with focused illumination*. NDT&E International 77 (2016) 28–34.

[17] Magnani FS, Silva RNTD. *Influence of the errors in an infrared camera on the estimation of thermal conductivity and thermal capacity of a gypsum plaster sample*. Infrared Phys Technol 2013;57:14-20. doi:10.1016/j.infrared.2012.11.004.

[18] Strzałkowski K, Dadarlat D, Streza M, Zakrzewski J. *Thermal characterization of ZnBeMnSe mixed compounds by means of photopyroelectric and lock-in thermography methods*. Appl Phys A 2015;119:1165-71. doi:10.1007/s00339-015-9086-3.

[19] Fuente R, Rodríguez S, Mendioroz A, Salazar A, Zhukov A, Zhukova V. *Thermal Conductivity and Diffusivity Measurements of Glass-Coated Magnetic Microwires Using Lock-in Thermography*. Int J Thermophys 2014;36:1137–41. doi:10.1007/s10765-014-1615-3.

iJETRM
International Journal of Engineering Technology Research & Management

[20] Incropera, F. P.; DeWitt D. P.; Bergman, T. L.; Lavine, A.S.; Incropera's *Principles of Heat and Mass Transfer*. John Wiley & Sons; Global Edition (2017) 1000p. ISBN-13: 978-1119382911
[21] Patience GS. *Experimental methods and instrumentation for chemical engineers*. Waltham MA: Elsevier; 2013.
[22] Ashby MF, Jones DRH. *Engineering materials 1: an introduction to properties, applications and design*. London: Elsevier; 2011, eBook ISBN: 9780080966663.
[23] Ursine W, Calado F, Teixeira G, Diniz H, Silvino S, Andrade RD. *Thermal/Visible Autonomous Stereo Visio System Calibration Methodology for Non-controlled Environments*. Proceedings of the 2012 International Conference on Quantitative InfraRed Thermography 2012. doi:10.21611/qirt.2012.261.